A&A 439, 1057–1060 (2005)
DOI: 10.1051/0004-6361:20042587


Astronomy & Astrophysics

# Envelope models for the supersoft X-ray emission of V1974 Cyg

G. Sala and M. Hernanz

Institut d'Estudis Espacials de Catalunya and Institut de Ciències de l'Espai (CSIC), Campus UAB, Facultat de Ciències, Torre C5-parell, 2a planta, 08193 Bellaterra (Barcelona), Spain
e-mail: [sala;hernanz]@ieec.uab.es

Received 29 December 2004 / Accepted 7 February 2005

**Abstract.** The evolution of the soft X-ray emission of V1974 Cyg has been simulated by a white dwarf envelope model with steady hydrogen burning. The comparison of the results obtained from ROSAT observations with the results of our envelope models indicates that the post-outburst evolution of the nova can be explained by steady H-burning on either a 0.9 $M_{\odot}$ white dwarf with 50% degree of mixing between solar-like accreted material and the ONe degenerate core, or on a 1.0 $M_{\odot}$ ONe white dwarf with 25% mixing.

**Key words.** stars: individual: V1974 Cygni – stars: novae, cataclysmic variables – stars: white dwarfs – X-rays: binaries

## 1. Introduction

V1974 Cyg (Nova Cygni 1992), discovered on 1992 February 19, was the first classical nova to be observed in all wavelengths, from radio to $\gamma$-rays. The P Cyg profiles found in all the UV resonance lines of the emission line spectra observed by IUE (Shore et al. 1993, 1994) and the strong [Ne III] $\lambda\lambda$3869, 3968 and [NeIV] $\lambda\lambda$3346, 3426 emission lines that dominated the nebular spectrum (Barger et al. 1993) established V1974 Cyg as a neon nova. V1974 Cyg was observed by ROSAT between 1992 April 22 and 1993 December 3 (Krautter et al. 1996). The X-ray light-curve showed three phases: a first rise phase up to day 255 after outburst, a plateau phase without great variation in flux from day 255 to 511, and a final and fast decline from day 511 to day 653 after outburst. During the plateau and decline phases, the X-ray spectrum was dominated by the soft photospheric emission, which was well fitted by MacDonald & Vennes (1991) ONe enhanced white dwarf atmosphere models (Balman et al. 1998).

Classical nova outbursts are caused by the explosive burning of hydrogen on the surface of a white dwarf in a cataclysmic variable. When a critical amount of H-rich material has been accumulated on the white dwarf surface, ignition in degenerate conditions takes place and thermonuclear runaway is initiated in the accreted layer. The envelope expands and a fraction of it is ejected at large velocities, while the rest returns to hydrostatic equilibrium and remains in steady nuclear burning with constant bolometric luminosity (Starrfield 1989). As the envelope expands, the photosphere recedes and the effective temperature increases, shifting the spectrum from optical through UV to soft X (MacDonald 1996; Krautter 2002). The soft X-ray emission, arising as the ejecta becomes optically thin to X-rays, is thus a direct indicator of the thermonuclear burning in the post-outburst white dwarf envelope. All novae are expected to undergo this phase, showing the spectrum of a hot white dwarf atmosphere (MacDonald & Vennes 1991), with effective temperatures in the range $10^5$–$10^6$ K and luminosities close to the Eddington limit. The duration of the soft X-ray emitting phase is expected to depend on the white dwarf mass and the envelope mass left after the outburst. Without any model of the post-outburst nova, it has been usually estimated as the nuclear time-scale of the envelope left, assumed to have a mass similar to the accreted layer needed to trigger the outburst, $\sim 10^{-4}$–$10^{-5}$ $M_{\odot}$, indicating nuclear time-scales of tens or hundreds of years (Starrfield 1989; MacDonald 1985).

Nevertheless, X-ray observations indicate much shorter turn-off times for classical novae. During the last decade, ROSAT observed a total of 39 novae less than 10 years after outburst, but only three were found to emit soft X-rays (Orio et al. 2001): V1974 Cyg 1992 (with turn-off 18 months after outburst; Krautter et al. 1996), GQ Mus 1983 (with turn-off 9 years after outburst; Ögelman et al. 1993; Shanley et al. 1995) and Nova LMC 1995 (still bright in the year 2000, when observed with XMM-Newton; Orio & Greiner 1999; Orio et al. 2003). Out of these three novae detected, the best observed one was V1974 Cyg, for which the whole evolution of the soft X-ray emission was followed.

Here we present a model for a post-outburst white dwarf envelope that can explain the evolution of the soft X-ray emission and turn-off of V1974 Cyg. Furthermore, from the comparison of the model with ROSAT observations, the white dwarf mass, envelope composition and envelope mass of V1974 Cyg are constrained.

## 2. White dwarf envelope models for V1974 Cyg

A numerical model has been developed to simulate the physical conditions in the steady hydrogen burning envelope of post-outburst novae. A grid of white dwarf envelope models has been computed for white dwarf masses from 0.9 to 1.3 $M_\odot$. Three compositions from José & Hernanz (1998) hydrodynamic nova models have been considered, corresponding to ONe novae with different degrees of mixing between the solar accreted matter and the degenerate core: ONe25 models, with 25% mixing (in mass fractions $X = 0.53$, $Y = 0.21$, $\delta X_{\rm O} = 0.13$ – extra O mass fraction beyond that in $Z$ –, $\delta X_{\rm Ne} = 0.08$ – extra Ne mass fraction –; $Z$ contains metals in solar fractions); ONe50, with 50% mixing ($X = 0.35$, $Y = 0.14$, $\delta X_{\rm O} = 0.26$, $\delta X_{\rm Ne} = 0.16$); and ONe75, with 75% mixing ($X = 0.18$, $Y = 0.08$, $\delta X_{\rm O} = 0.38$, $\delta X_{\rm Ne} = 0.24$). Evolution is approximated as a sequence of steady state models (for a description of the envelope models see Sala & Hernanz 2005).

The results show that an envelope with steady H-burning proceeds along a plateau of quasi-constant luminosity, shrinking its photospheric radius as the envelope mass is reduced, and increasing its effective temperature as the photosphere sinks into deeper and hotter layers of the envelope. The average plateau luminosity increases for increasing white dwarf masses and for decreasing hydrogen abundances, according to the expression $L(L_\odot) \simeq 5.95 \times 10^4 \left(\frac{M}{M_\odot} - 0.536X - 0.14\right)$. Thermonuclear reactions continue until the envelope mass is reduced to the minimum critical mass for stable hydrogen burning, which occurs shortly after the maximum effective temperature is reached. Since no equilibrium configuration for a smaller envelope mass exists, the shell sources turn-off and the white dwarf starts to cool down. The upper panel in Fig. 1 shows the photospheric radius versus the effective temperature for some of our models. The lower panels show the envelope mass for the same models, with the time intervals, in days, spent by the envelopes in evolving between adjacent points.

For the comparison of our models with V1974 Cyg, results from Table 1 in Balman et al. (1998) have been used (see Table 1). For each observation, they obtained a $3\sigma$ confidence range for all model parameters, including the effective temperature and the atmosphere normalization constant, defined as $(R/D)^2$, where $R$ is the photospheric radius and $D$ is the distance to the source. Several determinations of the distance to V1974 Cyg can be found in the literature (Quirrenbach et al. 1993; Shore et al. 1994; Paresce et al. 1995; Chochol et al. 1997; Balman et al. 1998; Cassatella et al. 2004). In this work, we adopt the mean value and the whole uncertainty derived from these distance determinations, 2.5 ± 0.8 kpc, to obtain the photospheric radius from the normalization constants listed in Table 1 of Balman et al. (1998). The contours resulting from this derived radius and the effective temperature range from Balman et al. (1998) are overplotted on our models in Fig. 1 (upper panel). The large uncertainty in the distance makes an analysis based on the photospheric radius rather unreliable. Nevertheless, the evolution of the effective temperature alone restricts the possible models for V1974 Cyg to very few, and makes our main results independent of the distance determination.

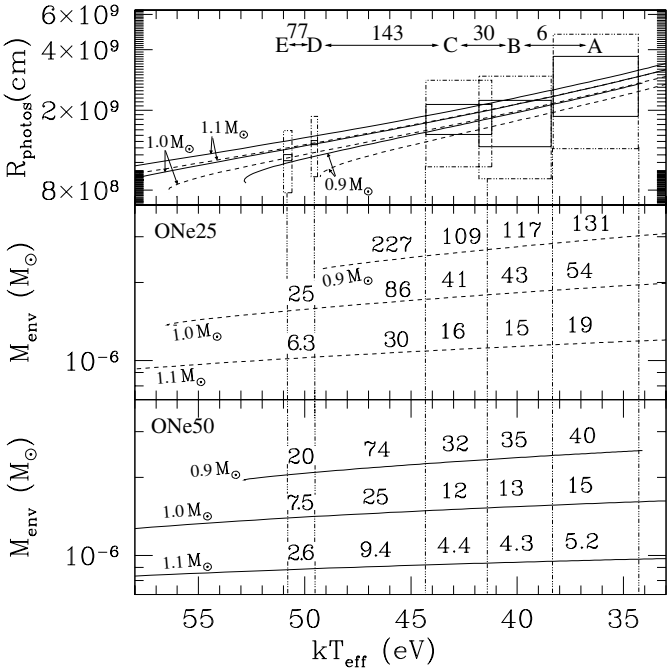


**Fig. 1.** Observational results for V1974 Cyg compared to our envelope models. *Upper panel*: spectral parameters (photospheric radius, $R_{\rm photos}$, and effective temperature, $kT_{\rm eff}$) for ROSAT observations on days 255(A), 261(B), 291(C), 434(D) and 511(E) after outburst (from Balman et al. 1998). Solid line contours for a distance of 2.5 kpc; dotted line contours for all the distance range of 1.7−3.3 kpc). Observational results are overplotted on ONe25 (dashed) and ONe50 (solid) envelope models, for white dwarf masses 0.9, 1.0 and 1.1 $M_\odot$. Numbers indicate days between observations. Vertical lines are orientative for comparison with the lower panels. *Middle panel*: envelope masses for ONe25 models. Numbers indicate days spent by the envelope model between two adjacent points. *Lower panel*: same as in middle panel for ONe50 models.

**Table 1.** ROSAT observational results for V1974 Cyg.

| | Day after outburst | $K^{a,b}$ $10^{-25}$ | $R^c_{\rm photos}$ ($10^9$ cm) | $kT^b_{\rm eff}$ (eV) |
|---|---|---|---|---|
| A | 255 | 0.6–2.4 | 1.8–3.7 | 34.3–38.3 |
| B | 261 | 0.3–0.9 | 1.3–2.3 | 38.4–41.8 |
| C | 291 | 0.4–0.8 | 1.5–2.1 | 41.2–44.3 |
| D | 434 | 0.32–0.36 | 1.3–1.4 | 49.4–49.7 |
| E | 511 | 0.22–0.26 | 1.1–1.2 | 50.6–51.0 |

[a] Normalization constant of the white dwarf atmosphere model, $K = (R/D)^2$, where $R$ and $D$ are the photospheric radius and the distance to the source.
[b] Results from Balman et al. (1998).
[c] Photospheric radius for a distance of 2.5 kpc.

### 2.1. Maximum effective temperature

A first distance-independent parameter to compare observations and models is the maximum effective temperature. According to Balman et al. (1998), the maximum effective

temperature observed by ROSAT was ∼50 eV, on day 511 after outburst. Nevertheless, the actual maximum temperature could have been missed by ROSAT, since no observations were performed between days 511 and 612. The V1974 Cyg X-ray light curve (Krautter et al. 1996) indicates that the end of the plateau phase, and therefore the maximum effective temperature, occurred between these two ROSAT observations. Furthermore, UV observations indicated that the hot central source had ceased to photoionize the ejecta at about day ∼ 530 after outburst (Shore et al. 1996). In this case, the actual maximum effective temperature should have been reached before day 530 and thus should be not much higher than the value obtained for day 511, ∼50 eV.

Taking into account this limit, we find that some envelope models are unlikely to represent the observed evolution: for the ONe75 models, any white dwarf more massive than 0.9 $M_\odot$ has an effective temperature higher than observed. For the ONe50 models, we find that only the 0.9 $M_\odot$ white dwarf envelopes have a good maximum effective temperature (53 eV, see Fig. 1). Finally, in the case of the ONe25 composition, this requirement could be fullfilled by a white dwarf of mass between 0.9 $M_\odot$ ($kT_{\max}$ = 49 eV) and 1.0 $M_\odot$ ($kT_{\max}$ = 56 eV). Nevertheless, since evolution at high effective temperatures could proceed faster than the time interval between observations, this criterion alone is not enough to reject models with maximum effective temperatures larger than observed. The evolution of the effective temperature adds more constrains.

### 2.2. Evolution of the effective temperature

The evolution of the effective temperature provides a second and more powerful distance-independent diagnostic tool. Only some combinations of core mas and envelope composition can reproduce the observed evolution. Interestingly enough, these cases are among the ones with good maximum effective temperature: 0.9 $M_\odot$ for ONe50 and 1.0 $M_\odot$ for ONe25. The days elapsed between ROSAT observations during the plateau phase are indicated in the upper panel in Fig. 1, and the corresponding time intervals for the models, in the lower panels. Table 2 lists the interval times for the models of each composition that could better fit the observed evolution. The time elapsed until day 511 should be taken with care: if the maximum effective temperature and the subsequent turn-off occurred close to that day, several factors can affect the evolution. It is possible that the X-ray observation took place shortly after reaching the maximum effective temperature, and not before. In this case, if the envelope was already starting to cool down, with still a high effective temperature, the luminosity and effective radius would have been slightly smaller than the corresponding values for the source still on, which could explain the fact that the photospheric radius on day 511 is smaller than predicted by models. The time estimated from the envelope models for evolution along the high luminosity branch would then be smaller than observed, and this is indeed the case for the envelope models with time-scales more similar to observations.

The ONe75 envelope models (with $X_{\rm H}$ = 0.18) cannot, in any case, simulate the observed evolution. Even for the smallest white dwarf in our grid (0.9 $M_\odot$, which is too small for an ONe white dwarf, according to stellar evolution models), the total time elapsed between effective temperatures corresponding to days 255 and 511 is ∼40 days, smaller than the 256 days elapsed between observations. For the ONe50 0.9 $M_\odot$ white dwarf envelope models, the time-scale for the same interval of effective temperatures (141−181 days) is closer to the observed one. Finally, time-scales for ONe25 1.0 $M_\odot$ models are also similar to the observed ones. In summary, the best candidates for V1974 Cyg are either a 0.9 $M_\odot$ white dwarf with 50% mixing (with $X$ = 0.35) or a 1.0 $M_\odot$ white dwarf with a 25% mixing (with $X$ = 0.53).

In both cases, the envelope mass is in the range $\sim 2 \times 10^{-6}$ $M_\odot$ (see low panels in Fig. 1) and the luminosity of the model is $\sim 3.5 \times 10^4$ $L_\odot$. Since the comparison with models is based on the effective temperature, this luminosity determination is independent of distance.

**Table 2.** Time intervals observed and simulated by envelope models.

| Days between observations | ONe75 0.9 $M_\odot$ | ONe50 0.9 $M_\odot$ | ONe25 1.0 $M_\odot$ |
|---|---|---|---|
| 256 (A–E) | 39.1–43.9 | 161–201 | 195–249 |
| 179 (A–D) | 34.1–38.9 | 141–181 | 170–224 |
| 6 (A–B) | <13.6 | <75 | <97 |
| 30 (B–C) | <17.1 | <67 | <84 |
| 143 (C–D) | 17–25.3 | 74–106 | 86–127 |
| 77 (D–E) | 5 | 20 | 25 |
| 36 (A–C) | 8.8–21.9 | 35–107 | 43–138 |
| 173 (B–D) | 25.3–34.1 | 106–141 | 127–170 |

## 3. Discussion

Among our two candidate envelope models, the 50% mixing case is favoured by independent determinations of the hydrogen mass fraction in the V1974 Cyg ejecta. Austin et al. (1996) found $X$ = 0.17 from optical and ultraviolet observations, which is similar to the hydrogen abundance in our ONe75 models ($X$ = 0.18). Nevertheless, as mentioned above, this model would imply a too fast evolution compared to ROSAT data. Using mid-infrared spectroscopy, Hayward et al. (1996) determined $X$ = 0.30, very close to the value in our ONe50 models. Later works (Moro-Martín et al. 2001; Vanlandigham et al. 2002) determined smaller metal enhancements than Austin et al. (1996), which also agrees with a hydrogen abundance higher than $X$ = 0.18.

In any of our candidate models, the white dwarf mass lies at the lower end of previous determinations. From their X-ray observations, Balman et al. (1998) used the mass-luminosity relation from Iben & Tutukov (1996) to find a white dwarf mass in the range 0.9−1.4 $M_\odot$. Krautter et al. (1996) estimated the star mass to be 1.25 $M_\odot$ using the mass-luminosity relation of Iben (1982), which is reproduced by our core-mass luminosity relation above for the hydrogen mass fraction of his

models, $X = 0.64$. They took the nova luminosity early in the outburst, $5 \times 10^4\ L_\odot$, determined by Shore et al. (1993, 1994), who assumed a distance of 3 kpc. Nevertheless, later distance determinations situated the nova closer than 3 kpc and thus the luminosity would be smaller, indicating a less massive white dwarf. Moreover, envelope models of Iben (1982) and Iben & Tutukov (1996) used in both previous mass determinations were hydrogen richer ($X = 0.64$) than our models, requiring a more massive white dwarf for the same luminosity. Our mass determination is in agreement with Retter et al. (1997), who estimated the mass of the white dwarf to be in the range $0.75-1.07\ M_\odot$ from the periodicities oberved in the light-curve and the precessing disc model for the superhump phenomenon. A factor cited in previous works (Austin et al. 1996) in favour of a massive white dwarf was the minimum mass for ONe degenerate cores, $\sim 1.2\ M_\odot$. Recent evolutionary calculations in Gil-Pons et al. (2003) have fixed a smaller lower limit, showing that final ONe white dwarfs in cataclysmic variables have typical masses between 1.0 and 1.1 $M_\odot$, thus including our 1.0 $M_\odot$ ONe25 model as a possible one according to stellar evolution.

The accreted mass to trigger the outburst of a 1 $M_\odot$ white dwarf with 50% mixing predicted by theoretical models is $\sim 6 \times 10^{-5}\ M_\odot$, whereas the ejected mass is $\sim 5 \times 10^{-5}\ M_\odot$ (José & Hernanz 1998). Therefore, models do not predict remnant envelope masses as low as those with steady hydrogen burning that can explain the soft X-ray emission observed for V1974 Cyg ($\sim 2 \times 10^{-6}\ M_\odot$). Since the evolution of V1974 Cyg from day 255 after outburst to the end of the constant bolometric luminosity phase can be explained solely as a result of pure hydrogen burning, there should be a mass-loss mechanism able to get rid of most of the envelope mass in around 8 months (Tuchman & Truran 1998), but acting at a much lower level later on. A mechanism such as a radiation driven wind (Kato & Hachisu 1994) approaches this, evolving from large to small rates as envelope mass is depleted; however, a fine tuning of various model parameters would be required to obtain the particular amount of mass-loss needed. Thus, it is not well known what mechanisms are responsible for the depletion of the envelope mass down to the levels required for the correct interpretation of the X-ray emission observed in V1974 Cyg.

*Acknowledgements.* This research has been partially funded by the MCYT project AYA2004-06290-C02-01 and by the EU FEDER funds. G.S. acknowledges a FPI grant from the MEC.

## References

Austin, S. J., Wagner, R. M., Starrfield, S., et al. 1996, AJ, 111, 2
Balman, S., Krautter, J., & Ögelman, H. 1998, ApJ, 499, 395
Barger, A. J., Gallagher, J. S., Bjorkman, K. S., Johansen, K. A., & Nordsieck, K. H. 1993, ApJ, 419, L85
Cassatella, A., Lamers, H. J. G. L. M., Rossi, C., Altamore, A., & Gonzalez-Riestra, R. 2004, A&A, 420, 571
Chochol, D., Grygar, J., Pribulla, T., et al. 1997, A&A, 318, 908
Gil-Pons, P., García-Berro, E., José, J., Hernanz, M., & Truran, J. W. 2003, A&A, 407, 1021
Hayward, T. L., Saizar, P., Gehrz, R. D., et al. 1996, ApJ, 469, 854
Iben, I., Jr. 1982, ApJ, 259, 244
Iben, I., Jr., & Tutukov, A. V. 1996, ApJS, 105, 145
José, J., & Hernanz, M. 1998, ApJ, 494, 680
Kato, M., & Hachisu, I. 1994, ApJ, 437, 802
Krautter, J. 2002, in Classical Nova Explosions, ed. M. Hernanz, & J. José, AIP Conf. Proc., 637, 345
Krautter, J., Ögelman, H., Starrfield, S., Wichmann, R., & Pfeffermann, E. 1996, ApJ, 456, 788
MacDonald, J. 1996, in Cataclysmic Variables and Related Objects (Dordrecht: Kluwer), 281
MacDonald, J., & Vennes, S. 1991, ApJ, 373, L51
MacDonald, J., Fujimoto, M. Y., & Truran, J. 1985, ApJ, 294, 263
Moro-Martín, A., Garnavich, P. M., & Noriega-Crespo, A. 2001, ApJ, 121, 1636
Ögelman, H., Orio, M., Krautter, J., & Starrfield, S. 1993, Nature, 361, 331
Orio, M., & Greiner, J. 1999, A&A, 344, L13
Orio, M., Covington, J., & Ögelman, H. 2001, A&A, 373, 542
Orio, M., Hartmann, W., Still, M., & Greiner, J. 2003, ApJ, 594, 435
Paresce, F., Livio, M., Hack, W., & Korista, K. 1995, A&A, 299, 823
Quirrenbach, A., Elias II, N. M., Mozurkewich, D., et al. 1993, AJ, 106, 1118
Retter, A., Leibowitz, E. M., & Ofek, E. O. 1997, MNRAS, 286, 745
Sala, G., & Hernanz, M. 2005, submitted
Shanley, L., Ögelman, H., Gallagher, J. S., Orio, M., & Krautter, J. 1995, ApJ, 438, L95
Shore, S. N., Starrfield, S., & Sonneborn, G. 1996, ApJ, 463, L21
Shore, S. N., Sonneborn, G., Starrfield, S., Gonzalez-Riestra, R., & Ake, T. B. 1993, AJ, 106, 2408
Shore, S. N., Sonneborn, G., Starrfield, S., Gonzalez-Riestra, R., & Polidan, R. S. 1994, ApJ, 421, 344
Starrfield, S. 1989, in Classical Novae (New York: Wiley), 39
Tuchman, Y., & Truran, J. W. 1998, ApJ, 503, 381
Vanlandingham, K. M., Starrfield, S., Shore, S. N., & Wagner, R. M. 2002, in Classical Nova Explosions, ed. M. Hernanz, & J. José, AIP Conf. Proc., 637, 224